

Research Space

Journal article

Influence of carbon source complexity on porosity, water retention and extracellular matrix composition of *Neurospora discreta* biofilms

Ahmed, A., Narayanan, R.A. and Veni, A.R.

*"This is the peer reviewed version of the following article: Ahmed, A., Narayanan, R. and Veni, A. (2020), Influence of carbon source complexity on porosity, water retention and extracellular matrix composition of *Neurospora discreta* biofilms. J Appl Microbiol, 128: 1099-1108. <https://doi.org/10.1111/jam.14539>, which has been published in final form at the above URL. This article may be used for non-commercial purposes in accordance with Wiley Terms and Conditions for Use of Self-Archived Versions."*

1 **Influence of carbon source complexity on porosity, water retention and extracellular**
2 **matrix composition of *Neurospora discreta* biofilms**

3

4 Asma Ahmed^{1*}, R. Aravinda Narayanan^{2a} and Abinaya Veni R^{2b}

5

6 **Author affiliations:**

7 ¹School of Human and Life Sciences,

8 Canterbury Christ Church University, North Holmes Road Canterbury, CT1 1QU, United Kingdom

9

10 ^{2a}Department of Physics, ^{2b}Department of Chemical Engineering

11 Birla Institute of Technology and Science (Pilani), Hyderabad campus,

12 Hyderabad - 500078, India

13

14 **Running Headline**

15 Effect of carbon source on *Neurospora discreta* biofilms

16

17 ***Corresponding author**

18 Asma Ahmed

19 School of Human and Life Sciences,

20 Canterbury Christ Church University, North Holmes Road Canterbury, CT1 1QU, United Kingdom

21 Email: asma.ahmed@canterbury.ac.uk

22

23 **Abstract**

24 **Aims:** To evaluate carbon source complexity as a process lever to impact the microstructure, chemical
25 composition and water retention capacity of biofilms produced by *Neurospora discreta*.

26 **Methods and Results:** Biofilms were produced by non-pathogenic fungus *N. discreta*, using sucrose,
27 cellulose or lignin as carbon source. Increase in complexity of carbon source from sucrose to lignin
28 resulted in decreased water retention values (WRV) and wet weights of harvested biofilms. Confocal
29 laser scanning microscopy (CLSM) was used to calculate porosity from bright field images, and relative
30 stained areas of cells and carbohydrates from fluorescence imaging of samples stained with Trypan blue
31 and Alexa Fluor 488. Porosity and relative quantity of cells increased with increase in carbon source
32 complexity while the amount of carbohydrates decreased. Chemical analysis of the extracted
33 extracellular matrix (ECM) showed that biofilms grown on more complex carbon sources had lower
34 carbohydrate and protein content, which also explains the lower WRV trend, as carbohydrates are
35 hydrophilic.

36 **Conclusions:** The nature of carbon source impacts the metabolic pathway of cells, thereby influencing
37 the relative proportions of ECM and cells. This in turn impacts the microstructure, composition and
38 water content of biofilms.

39 **Significance and Impact of the Study:** This work shows that carbon source can be used as process lever
40 to control the properties of biofilms and presents a novel view of biofilms as potentially useful
41 biomaterials.

42

43

44

45 Introduction

46 Worldwide public health and environmental concerns with synthetic polymers have led to a growing
47 interest in biologically produced materials that are natural, renewable as well as biodegradable (Cole *et*
48 *al.* 2011; Webb *et al.* 2013). This class of biomaterials include biocomposites based on wood and natural
49 fibers such as cellulose, as well as microbially produced biopolymers. Microbial biopolymers produced
50 by bacteria and fungi have an added advantage of process control and scalability as these can be
51 produced in bioreactors: Examples include pullulan, bacterial cellulose, scleroglucan, xanthan, poly-3-
52 hydroxybutyrate and exopolysaccharides (EPS) (Survase *et al.* 2007; Mohammadkazemi *et al.* 2015; Jiang
53 *et al.* 2016; Majee *et al.* 2017; Girometta *et al.* 2019). Due to the diversity in their properties, these
54 materials find application in various areas, being used as emulsifiers, stabilizers, gums, or for making
55 biocomposites. A well-researched example is microbial cellulose produced by various bacterial species,
56 which finds application in the food and medical industries as an additive, wound dressing material,
57 packaging material, etc. (Raghunathan 2013; Mohammadkazemi *et al.* 2015). However, nearly all of
58 these polymers are secreted by cells in soluble form, and require further downstream processing such as
59 precipitation, purification and fabrication (Lee *et al.* 2009). A few recent studies have demonstrated the
60 formation of solid fungal composites, which are formed by fungal mycelia grown on solid substrates
61 such as cotton, straw, hemp, and sawdust (Elsacker *et al.* 2019; Girometta *et al.* 2019). Wood-decay
62 fungi can penetrate these substrates, degrade the lignocellulosic components present, and eventually
63 replace the substrate with fungal biomass resulting in mycelium-based bio-composites (Girometta *et al.*
64 2019). Appels *et al.* (2019) found that the fungal species as well as the substrate used, significantly
65 impact the strength and stiffness of such bio-composites. More recently, hybrid composites made of
66 wood, cellulose nanofibrils and fungal mycelia were reported (Sun *et al.* 2019,). Most of these fungal
67 composites that form on solid substrates require further processing such as cold-pressing or curing at

68 high temperatures to achieve the mechanical strength required for their potential applications (Iordache
69 *et al.* 2018; Girometta *et al.* 2019).

70 A relatively unexplored area in biomaterials research is the evaluation of 'biofilms' as useful materials.
71 Biofilms are biological structures formed by microorganisms on various surfaces and interfaces,
72 consisting of communities of cells embedded in a self-produced extracellular polymeric matrix (ECM)
73 (Flemming and Wingender 2010). Owing to the detrimental effects of certain types of biofilms on
74 medical and industrial equipment, research on biofilms has largely focused on their detection,
75 prevention and removal (Francolini and Donelli 2010). On the other hand, biofilms formed in
76 wastewater treatment plants are considered advantageous as they help in degradation and removal of
77 contaminants, and provide a suitable habitat for the microorganisms involved in the process (Singh *et al.*
78 2006). In addition to immobilizing and housing cells, the purpose of biofilms is to enable cell-cell
79 interactions, retention of extracellular enzymes, and transport of nutrients and waste products to and
80 from the cells. This requires an intricate 3-dimensional structure, with varying pore sizes as well as an
81 amphiphilic nature for selective transport. The result is a highly porous, viscoelastic material with the
82 capacity to hold large amounts of water. Therefore, biofilms formed by non-pathogenic microorganisms
83 can be viewed as renewable, biodegradable and sustainable porous biomaterials with potential
84 applications as biological membranes. The main difference between biofilms and other microbial
85 biopolymers is that biofilms are formed as intact materials that would not need further purification or
86 downstream processing. Identification of parameters that can be used as process levers to tune the key
87 properties of biofilms could therefore pave the way for a new area of biomaterials research.

88 Several physical factors such as pH, temperature and fluid shear stress influence the biofilm mode of
89 life: We recently demonstrated that agitation of the growth reactor significantly impacts the
90 microstructure and the mechanical properties of biofilms (Narayanan and Ahmed 2019). Among the

91 chemical factors that are critical to cell growth and biofilm formation are the nutrients available in the
92 surrounding medium. Within the nutrient medium, the nature and quantity of carbon source have a
93 profound influence on biofilm formation (Ellis *et al.* 2000; Wawrik *et al.* 2005; Ib and Chauhan 2015),
94 and can be used as levers to control the structure and mechanical properties of biofilms, which would
95 have a direct bearing on their applications.

96 This work pertains to biofilms formed by a locally isolated strain of non-pathogenic fungus, *Neurospora*
97 *discreta*, on the air-liquid interface. When grown in liquid medium, *N. discreta* rapidly forms a biofilm on
98 the surface of the medium, layer by layer, eventually forming a bio-composite of cells and ECM
99 comprising carbohydrates, proteins, lipids and other polymeric substances. The intricate and interwoven
100 matrix structure results in highly porous biofilms that hold >90% water by weight and the presence of
101 the thick filaments of *N. discreta* reinforces the biofilms making them strong enough to be harvested
102 and tested in an intact condition. The objective of the present work was to evaluate the effect of carbon
103 source complexity on the properties of biofilms formed by *N. discreta*. Three carbon sources were tested
104 in this study: (1) sucrose, a disaccharide of glucose and fructose, and a common carbon source in used in
105 microbial growth media due to the ease of degradation, (2) cellulose, a natural plant-derived polymer
106 and a polysaccharide of β -glucose units with 1,4-glycosidic linkages and (3) lignin, a bulky and
107 recalcitrant phenolic polymer, consisting of several methoxylated derivatives of benzene
108 (phenylpropanoid alcohols, also called monolignols). Lignin is a common by-product of biorefineries
109 based on lignocellulosic biomass as well as paper and pulp industries and is metabolized by very few
110 organisms, including white rot fungi such as *Phanaerochaete chrysosporium* (Boyle *et al.* 1992), as well
111 as ascomycetes such as *N. discreta* (Pamidipati and Ahmed 2017). These carbon sources were selected
112 as they represent three levels of relative complexity in structure, and differ in their molecular weights –
113 all of which results in differences in how they are incorporated into the metabolic pathways of the

114 fungus. The biofilms formed from each of these carbon sources were analyzed in terms of their
115 microstructure as well as chemical composition.

116 A look into the common metabolic pathways of microorganisms shows that simpler carbohydrates such
117 as glucose or fructose are readily incorporated into the glycolytic pathway while a more complex
118 polysaccharide needs to be broken down into simpler units before it can join one of the catabolic
119 pathways. This results in differences in net ATP production, impacting the rate of cell growth as well as
120 the nature and amounts of products released by cells. As the formation of biofilms is a direct function of
121 cellular metabolism, we hypothesize that the complexity of the carbon source has a significant impact
122 on biofilm composition, which in turn would influence other key properties of the material, such as
123 porosity and the capacity to hold water. In the literature, the effect of carbon source on biofilm
124 formation and ECM secretion has been reported (Xu *et al.* 2017; Turskaya *et al.* 2018), but its impact on
125 physical, structural and chemical properties of biofilms has not been explored so far.

126 This work also introduces a new view of 'biofilms' as potentially useful biomaterials, in contrast to the
127 vast literature on biofilms formed by pathogenic microorganisms responsible for diseases and industrial
128 fouling. This is possible due to three reasons: first, *N. discreta* is a non-pathogenic and safe
129 microorganism (Perkins and Davis 2000); second, the biofilms formed are strong enough to be harvested
130 and handled as intact materials, possibly owing to the reinforcement provided by the long and thick
131 hyphae of *N. discreta* as the biofilm grows; third, the biofilms have a membranous porous structure.
132 Another unique feature of these biomaterials is that the formation on the air-liquid interface further
133 contributes to ease of harvesting without damaging the structure.

134

135 **Materials and Methods**

136 **Microorganism growth and maintenance**

137 *Neurospora discreta*, isolated locally from the bark of a Subabul wood tree (Pamidipati and Ahmed
138 2017) was used for producing biofilms. *N. discreta* was maintained on potato dextrose agar plates (PDA)
139 on which it grows as long filaments and produces abundant spores. The streaked plates were incubated
140 for 3-4 days at 28-30°C, after which the plates were refrigerated at 2-4°C until further use.

141

142 **Biofilm growth and harvest**

143 Biofilms were grown in 250 ml Erlenmeyer flasks containing 100 ml Vogel's medium (Vogel 1964) with
144 2% total carbon source at an initial pH of 5.6 ± 0.2 . For cellulose and lignin, this was added as 1.5%
145 carbon source plus 0.5% sucrose: The latter was added to initiate cell growth. The flasks containing the
146 culture medium were sterilized in an autoclave at 121°C for 15 minutes. Once the medium cooled, 0.1%
147 solution of filter sterilized biotin was added to each flask.

148 For inoculation of the flasks, cells of *N. discreta* grown on PDA were gently scraped and suspended into a
149 few ml of sterile Vogel's minimal medium. The suspension was then filtered through a coarse muslin
150 cloth to remove filaments and residual agar and the filtered spore suspension was used to inoculate the
151 flasks and mixed thoroughly to obtain a spore count of ~0.2 million cells/ml in each flask. After the initial
152 mixing, the flasks were incubated at 30°C for 7 days without any agitation.

153 The first layer of the biofilm is formed about a day after inoculation after which it thickens by adding
154 more layers. The biofilms were harvested by carefully removing them from the flasks using a long
155 spatula and placing them on a filter paper for a few minutes to drain excess medium. The wet weights
156 were then noted and the samples were sprayed with isopropyl alcohol to arrest further cell growth and
157 then refrigerated in petri dishes at 2-4°C until further analysis.

158 **Water Retention Value (WRV) and Dry weights**

159 A modified standard protocol from Tappi UM 256 (Cheng *et al.* 2010) was used to calculate the WRV of
160 the biofilms. For this, a known amount of sample was soaked in water for an hour and then centrifuged
161 at 1217 g for 15 minutes. Excess water was then removed and the sample was dried at 103.5 °C until
162 constant weight was achieved. The dry weight was then noted and the ratio of the difference in wet and
163 dry weights to the wet weight gave the WRV for each sample. Normalized dry weights were also
164 calculated by dividing the dry weight by the wet weight of each sample.

165

166 **Confocal Laser Scanning Microscopy**

167 Porosity measurement

168 Biofilm samples were imaged using confocal laser scanning microscopy (CLSM) (Leica DMI8 inverted
169 microscope) after drying at 30°C for about 3 hours. The samples auto-fluoresce which was used to
170 obtain bright field images with a 40X oil objective with z-step of 1 µm. From the bright field images
171 porosity is calculated which is a measure of structural heterogeneity in biofilms: It is defined as the ratio
172 of pore volume to biomass volume. The images were processed using ImageJ (Fiji) software. This
173 entailed converting each image into a grey-scale binary image and segmenting the image by consistently
174 applying a thresholding algorithm (Huang and Wang 1995)

175 The formula used for calculating porosity from confocal images is as follows:

176
$$\text{Porosity} = \frac{(\text{Field of view}) \times \sum(\text{Areal porosity} \times \text{Slice thickness})}{(\text{Volume of the sample})}$$

177 Where,
$$\text{Areal porosity} = \frac{\text{Number of void pixels}}{\text{Total number of pixels}}$$

178 Sample staining:

179 Samples were stained for fluorescence imaging to quantify carbohydrates and cells. Trypan Blue was
180 used to image the cells and Alexa Fluor 488 to image the carbohydrates (Zinchuk and Zinchuk 2008). For
181 this purpose, a small strip of each sample was first washed in phosphate buffer saline (PBS) solution,
182 after which 2000 μ l of diluted Trypan blue stain (1:1500) was added to the sample and incubated for 30
183 minutes. After incubation, the sample was washed again with PBS and excess stain was removed using
184 blotting paper. The film was then added to a well containing 200 μ l of 15 μ g/ml of Alexa Fluor 488 and
185 incubated for 30 minutes. The concentrations of both stains were decided based on experiments that
186 were designed to determine stain concentrations for which the stained areas were independent of
187 sample thickness. Finally, the sample was washed again with PBS buffer and the excess stain was
188 removed by using blotting paper. The film was then placed in a microscopic slide covered with a
189 coverslip and dried at 35 $^{\circ}$ C before viewing in the fluorescence mode of the CLSM. The stained area for
190 each stain was obtained using the software, and the stained volume was calculated using the number of
191 slices. A feature of the fluorescent imaging protocol that we adopted is that information about
192 carbohydrates and cells were obtained from the same area of the sample as the sample contained both
193 the stains.

194

195 **ECM extraction and analysis of composition**

196 ECM was extracted from the samples and analysed for carbohydrate and protein content. For extraction
197 we tried physical methods of centrifugation and ultrasonication. However, we report results only from
198 the chemical extraction method that used a combination of formaldehyde and sodium chloride as it
199 gave the highest yields (Jiao *et al.* 2010; Pan *et al.* 2010; Hemme 2015; Chiba *et al.* 2016).

200 The biofilms samples were soaked in 25 ml of 8.5% sodium chloride and 0.22% formaldehyde for 2
201 hours, then centrifuged and washed. The extracted EPS was then subjected to carbohydrate and protein
202 estimation. Lowry's protocol was used to measure the protein content in the extracted EPS (Lowry *et al.*
203 1951). Carbohydrate analysis involved acid hydrolysis of the EPS using 98% sulfuric acid for 2 hours,
204 followed by dilution to 4% and then autoclaving at 121°C for 1 hour. The samples were then cooled,
205 neutralized using 1N NaOH and the resulting sugars from the hydrolysis were measured using DNS
206 reagent (Miller 1959).

207 **Results**

208 **Biofilm growth, weights and water retention**

209 In all flasks, biofilm growth started 18-24 hours after inoculation. Biofilms formed on the air-liquid
210 interface and grew layer by layer each day for about 5 days after which there was no more visible
211 increase in thickness. Biofilms grown on lignin were considerably thinner and more fragile compared to
212 those grown on sucrose. Cellulose-grown biofilms were thicker than the lignin-grown ones but not as
213 thick as the sucrose-grown biofilms. This was also reflected in the wet weights, as shown in table 1. As
214 the carbon source complexity increased, the overall wet weight of the biofilm decreased. While this may
215 appear to be an expected trend, owing to the ease of degradability of the carbon source, which would
216 lead to greater cell growth in sucrose compared to lignin, the normalized dry weights (table 1) show the
217 opposite trend with lignin-grown biofilm being the highest and sucrose-grown biofilm the least. These
218 results indicate that the higher wet weight of sucrose-grown biofilms is due to the water held in the
219 sample and not because of greater amounts of biomass. This can also be seen from the WRV, which is
220 highest in sucrose-grown and lowest in lignin-grown biofilms. From these results it be concluded that
221 water content is controlled by the carbon source, which has implications for the microstructure of the

222 biofilms formed. WRV is an important property of biomaterials as it provides insight into the hydrophilic
223 nature and swelling capacity of the material (Cheng *et al.* 2010).

224

225 **Porosity and stained areas of biofilms**

226 Biofilms samples were dried and subjected to brightfield imaging using CLSM to determine the effect of
227 carbon source on the microstructure and more specifically the porosity. Each biofilm layer consists of
228 crisscrossing filamentous cells and ECM (Fig 1a) interspersed with pores (Fig 1b). The relative amounts of
229 cells and carbohydrates in ECM as a function of carbon source can be seen qualitatively from the stained
230 CLSM images in figure 2 and quantitatively from the plot of average stained areas in figure 3a. Analysis
231 of the bright field images yielded average values of porosity and filament diameter of biofilms grown on
232 each carbon source (Fig 3b). Sucrose-grown films contained the highest amount of carbohydrates and
233 lowest amount of cells, while lignin-grown films displayed the opposite trend. This can also explain the
234 trends in WRV (table 1), as carbohydrates are hydrophilic and therefore, higher the proportion of
235 carbohydrates, greater the amount of water held by the biofilms. Therefore, sucrose-grown biofilms,
236 which had relatively the highest carbohydrate content also had the highest WRV, and consequently the
237 highest wet weights. Another quantity that we can deduce from the average stained areas is the amount
238 of carbohydrates produced per cell which varied significantly across carbon sources. The ratios of
239 carbohydrates to cells yields values of 1.3 for sucrose, 0.8 for cellulose and only 0.3 for lignin, indicating
240 a difference in cellular metabolism in each case. When grown on sucrose, the metabolic energy seems
241 to be diverted towards carbohydrate production rather than cell growth, whereas growth on lignin
242 promotes cell growth much more significantly compared to carbohydrate production.

243 The porosity in sucrose-grown biofilms was the lowest while that in lignin-grown biofilms the highest.

244 The space between crisscrossing network of the hyphae – filamentous cells (figure 1) define the

245 micropores. The ECM grows around the cells and consequently, extends into the space between the
246 cells. Therefore, for lignin-grown biofilms for which ratio of carbohydrates to cells is only 0.3, the
247 porosity is nearly 75% in contrast to sucrose-grown biofilms whose porosity is less than 50% for which
248 the ratio of carbohydrates to cells is 1.3. Sucrose-grown biofilms also have higher filament diameter
249 compared to lignin-grown biofilms (Fig. 3b), which also indicates basic differences in the metabolism. In
250 all cases, the values of the cellulose-grown biofilms fell between the two extremes of sucrose and lignin,
251 showing increasing and decreasing trends of parameters with complexity of the carbon source.

252

253 **Chemical analysis**

254 Further insight into the effect of carbon source on the composition of ECM was obtained by extracting
255 the ECM and determining its carbohydrate and protein content, as these are the two main constituents
256 of ECM. Among other functions, proteins promote enzymatic activity that is necessary for 'digestion of
257 exogenous macromolecules for nutrient acquisition' (Flemming and Wingender 2010). As seen from
258 figure 4, the relative amounts of carbohydrates and proteins in the ECM decreased with increasing
259 complexity of carbon source. This data corroborates the trends seen in the CLSM analysis, and shows
260 that the amount of carbohydrates in the ECM of sucrose-grown films was the highest and that in lignin-
261 grown films the lowest.

262

263 **Discussion**

264 There is contradicting evidence in the literature on whether ECM production is a growth-associated or
265 non-growth associated process, as some researchers report that microorganisms produce less ECM
266 during the active growth phase, while others report that there is a linear positive relationship between

267 cell growth and ECM production (Laspidou and Rittmann 2002). From the results of this study, it can be
268 inferred that as the complexity of the carbon source increases from sucrose to lignin, the metabolism
269 seems to favor cell growth over ECM production, resulting in biofilms with lower water-holding capacity.
270 This can be explained by the differences in the manner in which carbon sources are metabolized by cells
271 for growth as well as ECM production (figure 5). Metabolism of sucrose involves its hydrolysis to glucose
272 and fructose. Glucose is phosphorylated to Glucose-1-phosphate and then to Glucose-6-phosphate,
273 which subsequently gets converted to Pyruvate after a series steps as shown in figure 5. Pyruvate serves
274 as a metabolic precursor to several other pathways and cycles including the TCA cycle for ATP
275 generation. The fructose produced from the hydrolysis of sucrose also gets phosphorylated and
276 eventually joins the glycolytic route. In a parallel pathway involving ECM production, Glucose-6-
277 phosphate or fructose-6-phosphate are converted to Uridine diphosphate (UDP)-Glucose or UDP-
278 galactose respectively, which eventually form repeating units that form the ECM (Ramos *et al.* 2001;
279 Tang and Ya-jie 2004; Chai *et al.* 2012. The production of ECM follows a biosynthetic pathway involving
280 the net consumption of ATP, rather than production of ATP. Therefore, when provided with an easily
281 degradable carbon source such as sucrose, the cells have sufficient ATP for growth, and therefore can
282 redirect the excess ATP to the anabolic steps involved in ECM production.

283 In case of cellulose, the polysaccharide is first broken down to cellodextrin, which then forms several
284 units of cellobiose that finally break down to glucose, which can then follow the same path described
285 above to form EPS or enter the glycolytic pathway. Therefore, the number of steps involved in
286 breakdown of cellulose are greater than those required for breakdown of sucrose and the net ATP
287 production would be lower as some would be consumed during breakdown of cellulose.

288 The degradation of lignin follows a completely different pathway compared to sucrose and cellulose,
289 involving breakdown of lignin via multiple steps to bi-aryls, and then to mono-aryls which over several

290 more steps go through ring cleavage and eventually form pyruvate, which can enter the TCA cycle
291 (Takayoshi 1986). Pyruvate can then either be utilized in the TCA cycle, or, under the right conditions
292 enter the gluconeogenesis pathway, leading to the formation of glucose. Some evidence in the literature
293 also exists on the presence of pyruvate itself in EPS. This means that the number of steps required for
294 metabolizing lignin are even greater compared to those required for cellulose and the net ATP
295 production and therefore the ATP available for producing ECM would be a lot lower compared to
296 simpler carbon sources. Therefore, the amount of ECM produced per cell in the case of lignin-grown
297 biofilms is a lot lower compared to that in sucrose-grown biofilms.

298 By impacting the composition of the biofilms, the complexity of the carbon source also influences the
299 physical properties of the biofilms, such as the capacity to retain water. As the ECM is largely composed
300 of carbohydrates, which are hydrophilic, the biofilms in which the relative amount of ECM is higher hold
301 more water, as seen from the higher WRV. Biofilms grown on lignin on the other hand, have a higher
302 proportion of cells that are less hydrophilic compared to ECM and therefore have lower WRV. The
303 presence of greater numbers of cells in these biofilms also leads to increased porosity as the pores are
304 formed by the crisscrossing of filamentous cells. Thus, complexity of carbon source could be an
305 important process lever to grow fungal biofilms with customized mechanical properties.

306 This work shows that the carbon source used has a significant impact on the composition of biofilms,
307 which in turn impacts the microstructure and the water-retention capacity. As the complexity of the
308 carbon source increased, water retention decreased due to the decreased levels of carbohydrates and
309 proteins. On the other hand, porosity increased with increasing complexity, owing to the presence of
310 more cells and less ECM. Based on these results, carbon source can be used as a process lever to tune
311 the porosity and composition of the biofilms, which would also have a direct bearing on the mechanical
312 properties. These biofilms are natural, biodegradable and sustainable materials that can find

313 applications as membranes for wastewater treatment (Shukla *et al.* 2014; Quilès *et al.* 2016), and wound
314 care materials (Smith *et al.* 2016; Suarato *et al.* 2018), which require flexible “housing” and a highly
315 porous structures for exchange of fluids.

316

317 **Acknowledgement**

318 The authors thank the central analytical lab facility at BITS Pilani, Hyderabad campus for access to
319 confocal microscopy.

320

321 **Conflict of Interest**

322 The authors declare that there is no conflict of interest.

323

324 **References**

325 Appels, F.V., Camere, S., Montalti, M., Karana, E., Jansen, K.M., Dijksterhuis, J., Krijgsheld, P. and
326 Wösten, H. A. (2019). Fabrication factors influencing mechanical, moisture- and water-related
327 properties of mycelium-based composites. *Mater Des* **161**, 64–71.

328 Fisher, B. and Fong, S. (2014). Lignin biodegradation and industrial implications. *AIMS Bioeng* **1**, 92–112.

329 Boyle, C. D., Kropp, B. R., and Reid, I. D. (1992). Solubilization and mineralization of lignin by white rot
330 fungi. *Appl Environ Microbiol* **58**, 3217–3224.

331 Chai, Y., Beauregard, P. B., Vlamakis, H., Losick, R., and Kolter, R. (2012). Galactose metabolism plays a

332 crucial role in biofilm formation by *Bacillus subtilis*. *MBio* **3**, e00184-12.

333 Cheng, Q., Wang, J., McNeel, J. F., and Jacobson, P. M. (2010). Water Retention Value Measurements of
334 Cellulosic Materials using a Centrifuge Technique. *BioResources* **5**, 1945–1954.

335 Chiba, A., Sugimoto, S., Sato, F., Hori, S., and Mizunoe, Y. (2016). A refined technique for extraction of
336 extracellular matrices from bacterial biofilms and its applicability. *Microb Biotechnol* **8**, 392–403.

337 Cole, M., Lindeque, P., Halsband, C., and Galloway, T. S. (2011). Microplastics as contaminants in the
338 marine environment : A review. *Mar Pollut Bull* **62**, 2588–2597.

339 Ellis, B. D., Butterfield, P., Jones, W. L., McFeters, G. A., and Camper, A. K. (2000). Effects of Carbon
340 Source, Carbon Concentration, and Chlorination on Growth Related Parameters of Heterotrophic
341 Biofilm Bacteria. *Microb Ecol* **38**, 330–347.

342 Elsacker, E., Vandeloock, S., Brancart, J., Peeters, E., and De Laet, L. (2019). Mechanical, physical and
343 chemical characterisation of mycelium-based composites with different types of lignocellulosic
344 substrates. *PLoS One* **14**, e0213954.

345 Flemming, H.-C., and Wingender, J. (2010). The biofilm matrix. *Nat Rev Microbiol* **8**, 623.

346 Francolini, I., and Donelli, G. (2010). Prevention and control of biofilm-based medical-device-related
347 infections. *FEMS Immunol. Med Microbiol* **59**, 227–238.

348 Girometta, C., Picco, A.M., Baiguera, R.M., Dondi, D., Babbini, S., Cartabia, M., Pellegrini, M. and Savino,
349 E. (2019). Physico-mechanical and thermodynamic properties of mycelium-based biocomposites :
350 A Review. *Sustainability* **11**, 1–22.

351 Hemme, C. L. (2015). Isolation of extracellular polymeric substances from biofilms of the
352 thermoacidophilic archaeon *Sulfolobus acidocaldarius*. *Front Bioeng Biotechnol* **3**, 1–11.

353 Huang, L., and Wang, M.-J. J. (1995). Image Thresholding by minimizing the measures of fuzziness. *Pattern*
354 *Recogn* **28**, 41–51.

355 Ib, P., and Chauhan, R. (2015). Effect of carbon and nitrogen sources on the growth , reproduction and
356 ligninolytic enzymes activity of *Dictyoarthrinium synnematicum somrith*. *Adv Zool Bot* **3**, 24–30.

357 Iordache, O., Perdum, E., Mitran, E. C., and Dumitrescu, I. (2018). Novel myco- composite material
358 obtained with *Fusarium Oxysporum*. *ICAMS 2018 - 7th International Conference on Advanced*
359 *Materials and Systems*, 111–116.

360 Jiao, Y., Cody, G. D., Harding, A. K., Wilmes, P., Schrenk, M., Wheeler, K. E., and Carolina, N. (2010).
361 Characterization of Extracellular Polymeric Substances from Acidophilic Microbial Biofilms. *Appl*
362 *Environ Microbiol* **76**, 2916–2922.

363 Lapidou, C. S., and Rittmann, B. E. (2002). A unified theory for extracellular polymeric substances ,
364 soluble microbial products , and active and inert biomass. *Water Res* **36**, 2711–2720.

365 Lee, K., Blaker, J. J., and Bismarck, A. (2009). Surface functionalisation of bacterial cellulose as the route
366 to produce green polylactide nanocomposites with improved properties. *Compos Sci Technol* **69**,
367 2724–2733.

368 Lowry, O. H., Rosebrough, N. J., Randall, R. J., and Lewis, A. (1951). Protein measurement with the folin
369 phenol reagent. *J Biol Chem* **193**, 265–275.

370 Majee, S. B., Avlani, D., and Biswas, G. R. (2017). Rheological Behavior and Pharmaceutical Applications
371 of Bacterial Exopolysaccharides. *J Appl Pharm Sci* **7**, 224–232.

372 Miller, G. L. (1959). Use of Dinitrosalicylic Acid Reagent for Determination of Reducing Sugar. *Anal Chem*
373 **31**, 426–428.

374 Mohammadkazemi, F., Azin, M., and Ashori, A. (2015). Production of bacterial cellulose using different
375 carbon sources and culture media. *Carbohydr Polym* **117**, 518–523.

376 Narayanan, R. A., and Ahmed, A. (2019). Arrested fungal biofilms as low-modulus structural bio-
377 composites: Water holds the key. *Eur Phys J E* **42**, 134–141.

378 Nelson, D., Cox, M., and Freeman, M. ed. (2004). *Lehninger Principles of Biochemistry, Fourth Edition*.

379 Pamidipati, S., and Ahmed, A. (2017). Degradation of Lignin in Agricultural Residues by locally Isolated
380 Fungus *Neurospora discreta*. *Appl Biochem Biotechnol* **181**, 1561–1572.

381 Pan, X., Liu, J., Zhang, D., Chen, X., Li, L., Song, W., and Yang, J. (2010). A comparison of five extraction
382 methods for extracellular polymeric substances (EPS) from biofilm by using three- dimensional
383 excitation-emission matrix (3DEEM) fluorescence spectroscopy. *WaterSA* **36**, 111–116.

384 Perkins, D. D., and Davis, R. H. (2000). Evidence for Safety of *Neurospora* Species for Academic and
385 Commercial Uses. *Appl Environ Microbiol* **66**, 5107–5109.

386 Quilès, F., Saadi, S., Francius, G., Bacharouche, J., and Humbert, F. (2016). In situ and real time
387 investigation of the evolution of a *Pseudomonas fluorescens* nascent bio film in the presence of
388 an antimicrobial peptide. *Biochim Biophys Acta* **1858**, 75–84.

389 Raghunathan, D. (2013). Production of Microbial Cellulose from the New Bacterial Strain Isolated From
390 Temple Wash Waters. *Int J Curr Microbiol App Sci* **2**, 275–290.

391 Ramos, A. N. A., Boels, I. C., Willem, M., and Santos, H. (2001). Relationship between Glycolysis and
392 Exopolysaccharide Biosynthesis in *Lactococcus lactis*. *Appl Environ Microbiol* **67**, 33–41.

393 Shukla, S. K., Mangwani, N., Rao, T. S., and Das, S. (2014). Biofilm-Mediated Bioremediation of Polycyclic
394 Aromatic Hydrocarbons. In *Microbial Biodegradation and Bioremediation*. Singh, R., Paul, D., and

395 Jain, R. K. (2006). Biofilms : implications in bioremediation. *Trends Microbiol* **14**, 389–397.

396 Smith, A. M., Moxon, S., & Morris, G. A. (2016). Biopolymers as wound healing materials. In *Wound*
397 *Healing Biomaterials* (Vol. 2). Elsevier Ltd.

398 Suarato, G., Bertorelli, R., and Athanassiou, A. (2018). Borrowing from nature: Biopolymers and
399 biocomposites as smart wound care materials. *Front Bioeng Biotechnol* **6**, 1–11.

400 Sun, W., Tajvidi, M., Hunt, C. G., McIntyre, G., and Gardner, D. J. (2019). Fully Bio-Based Hybrid
401 Composites Made of Wood, Fungal Mycelium and Cellulose Nanofibrils. *Sci Rep* **9**, 1–12.

402 Survase, S. A., Saudagar, P. S., Bajaj, I. B., and Singhal, R. S. (2007). Scleroglucan : Fermentative
403 Production , Downstream Processing and Applications. *Food Technol Biotechnol* **45**, 107–118.

404 Takayoshi, H. (1986). Catabolic Pathways and Role of Ligninases for the Degradation of Lignin
405 Substructure Models by White-Rot Fungi. *Wood Res* **73**, 58–81.

406 Tang, J., and Ya-jie, Z. (2004). Submerged Cultivation of Medicinal Mushrooms for Production of
407 Valuable Bioactive Metabolites. *Adv Biochem Eng Biotechnol* **87**, 25–59.

408 Turskaya, A. L., Uldanova, A. A., V, S. A., Bukin, Y. S., Verkhoturov, V. V, Gaida, B. K., and Markova, Y. A.
409 (2018). Formation of *Pectobacterium carotovorum* Biofilms Depending of the Carbon Source.
410 *Microbiology* **86**, 49–55.

411 Vogel, H. J. (1964). Distribution of Lysine Pathways Among Fungi: Evolutionary Implications. *Am Nat*
412 **XCVIII**, 435–446.

413 Wawrik, B., Kerkhof, L., Kukor, J., and Zylstra, G. (2005). Effect of Different Carbon Sources on
414 Community Composition of Bacterial Enrichments from Soil. *Appl Environ Microbiol* **71**, 6776–6783.

415 Webb, H. K., Arnott, J., Crawford, R. J., and Ivanova, E. P. (2013). Plastic Degradation and Its
416 Environmental Implications with Special Reference to Poly(ethylene terephthalate). *Polymers*
417 (*Basel*) **5**, 1–18.

418 Xu, C., Yu, J., Zhao, S., Wu, S., He, P., Jia, X., Liu, Y. and Mao, D. (2017). Effect of carbon source on
419 production , characterization and bioactivity of exopolysaccharide produced by *Phellinus vaninii*
420 Ljup. *An Acad Bras Cienc* **89**, 2033–2041.

421 Zinchuk, V., and Zinchuk, O. (2008). Quantitative Colocalization Analysis of Confocal Fluorescence
422 Microscopy Images. *Curr Protoc Cell Biol* **4**, 1–16.

423

424

425

426

427

428

429

430

431

432

433

434 **Table and Table Legend**

435

436 **Table 1.** Listing of various parameters that characterizes the water content in the biofilms grown with
437 different carbon sources

438

Carbon source	Wet weight (g)	WRV (g/g)	Normalized dry weight (g/g)
Sucrose	12.4 ± 0.5	98.9	0.011
Cellulose	11.1 ± 0.5	98.1	0.019
Lignin	6.9 ± 0.4	97.2	0.028

439

440

441 **Figure Legends**

442 **Fig. 1 (a)** Representative bright field image of a biofilm sample which shows the crisscrossing filaments
443 and resulting pores. **1(b)** Reconstructed 3-d image of a biofilm sample which shows the porous
444 structure.

445 **Fig. 2** CLSM images of biofilm samples grown on sucrose, cellulose and lignin. Samples were stained with
446 Alexa Fluor 488 for carbohydrates (top) and trypan blue for cells (bottom).

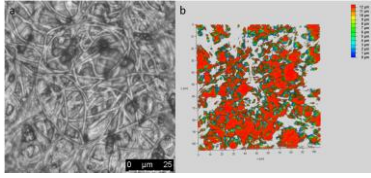
447 **Fig. 3 (a)** Average stained areas for cells (shaded) and carbohydrates (unshaded) and obtained from
448 CLSM images, **3(b)** Filament diameter (●) and porosity values (■) of biofilms grown on sucrose, cellulose
449 and lignin.

450 **Fig. 4** Carbohydrate and protein content in ECM of biofilms grown on sucrose, cellulose and lignin.

451 **Fig. 5** Summary of the metabolic pathways involved in breaking down sucrose, cellulose and lignin and
452 production of ECM. Adapted from multiple sources (Takayoshi 1986; Nelson *et al.* 2004; Fisher, B. and
453 Fong, S. 2014). Dashed lines represent multiple steps.

454

455

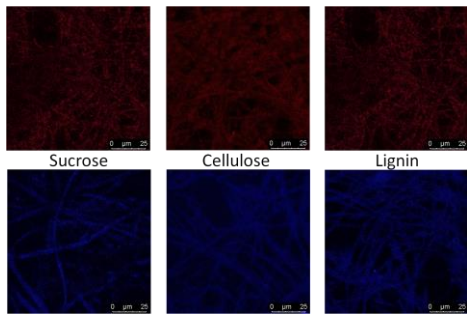


456

457 Figure 1

458

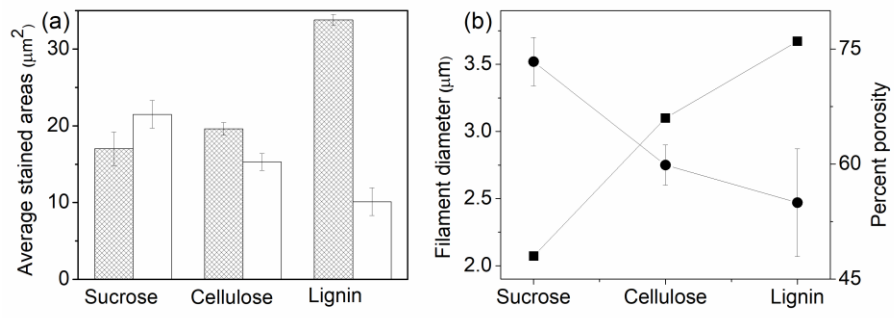
459



460

461 Figure 2

462

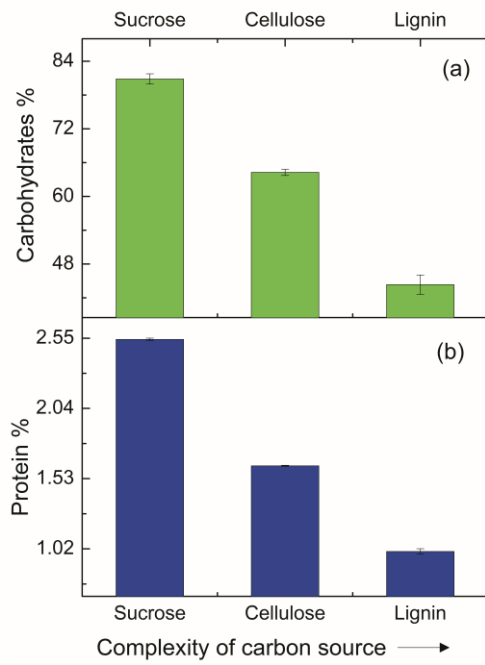


463

464 Figure 3

465

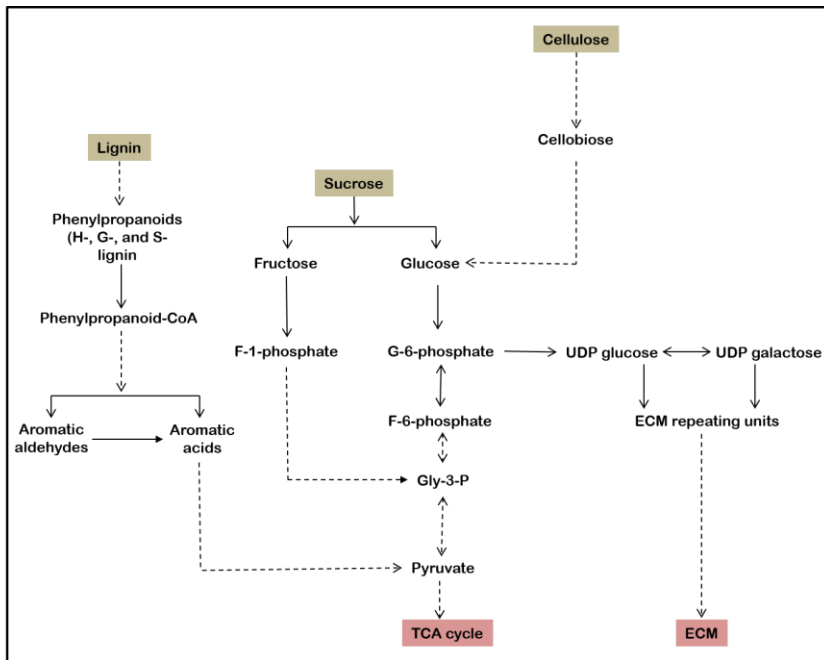
466



467

468 Figure 4

469



470

471 Figure 5